Wave Motion 83 (2018) 80–93

Contents lists available at ScienceDirect

Wave Motion

journal homepage: www.elsevier.com/locate/wamot

Dispersion curves of infinite laminate panels through a modal analysis of finite cylinders

F. Errico [a,b,*], S. De Rosa [b], M. Ichchou [a], F. Franco [b], O. Bareille [a]

[a] LTDS, Laboratoire de Tribologie et Dynamique des Systems, Ecole Centrale de Lyon, France

[b] pasta-lab, Laboratory for Promoting experiences in Aeronautical STructures and Acoustics, Dipartimento di Ingegneria Industriale - Sezione Aerospaziale, Universita di Napoli Federico II, Italy

HIGHLIGHTS

- This work presents an approach to predict the elastic waves in infinite, isotropic or composite, panels performing a modal analysis on an equivalent finite cylindrical model.
- An analogy, between the classical topologies of a straight line and a circumference, is exploited and tested.
- Different aspects, concerning the wave-mode duality, discretization and curvature, are investigated to frame the problem and test the robustness of the methodology.
- The analysis presents a well conditioned problem and solution for any propagation wave angle by transforming the original problem into a real modal analysis.

ARTICLE INFO

Article history:
Received 18 January 2018
Received in revised form 18 May 2018
Accepted 2 August 2018
Available online xxxx

Keywords:
Wave propagation
Dispersion curves
Modal analysis
Composite structures

ABSTRACT

This work presents an approach for using a modal analysis on an equivalent finite cylindrical model, to predict the elastic waves in infinite, isotropic or composite, panels. In the description of the infinite paths, an analogy, between the classical topologies of a straight line and a circumference, is exploited and tested. Different aspects, concerning the wave-mode duality and the discretization and the needed radii of curvature, are investigated to frame the problem and test the robustness of the methodology. The analysis presents a well conditioned problem and solution for any propagation wave angle by transforming the original problem into a simple modal analysis.

1. Introduction

The correct knowledge of how elastic waves freely behave inside a specific structure is mandatory for a correct modelling and analysis of the structure itself. Moreover, the generally frequency-dependent wavelengths, to be described in the modelling phase, must be known in advance for a correct discretization of the model. In FEA (Finite Element Analysis) [1], the knowledge of the wavelength is absolutely mandatory for the mesh sizing and for selecting the proper elements in the frequency range of analysis; in SEA, [2], detailed information about the group velocity and the modal density are necessary for the characterization of the specific subsystem and to analyse the energy exchange among them.

For an isotropic and homogeneous panel, three wave types are, present: bending, shear and longitudinal waves. An analytic procedure is available in literature for the corresponding wavenumbers, assuming the Kirchhoff–Love plate

* Corresponding author.
E-mail address: fabrizio.errico@ec-lyon.fr (F. Errico).

https://doi.org/10.1016/j.wavemoti.2018.08.007

Nomenclature

A	Cross-sectional area
D	Flexural stiffness of the plate
E	Young Modulus
G	Shear Modulus
I	Area moment of inertia
R	Cylinder radius
c_b	Bending wave speed
i	Circumferential modal order
k_b	Bending wavenumber
k_l	Longitudinal wavenumber
k_n	Wavenumber associated to the wavetype n
k_s	Shear wavenumber
u	Displacements along plate X direction
v	Displacements along plate Y direction
w	Displacements along plate Z direction
$\mathbf{A}$	Matrix of the extensional stiffness of the plate
$\mathbf{B}$	Matrix of the in-plane/flexural coupling laminate moduli
$\mathbf{D}$	Matrix of the flexural stiffness of the plate
$\mathbf{K}$	Stiffness matrix
$\mathbf{M}$	Mass matrix
$\mathbf{M}_l$	Matrix of the moments per unit length
$\mathbf{N}$	Matrix of the shearing forces per unit length
$\mathbf{q}$	Nodal vector of degrees of freedom
Γ	Wavefield linked to the target field variable
ρ_s	Density per unit area
$\boldsymbol{\epsilon}_0$	Strains of the middle plane of the plate
$\boldsymbol{\gamma}_0$	Curvatures of the plate
λ_i	Wavelength of the circumferential mode of order i
ν	Poisson ratio
ρ	Mass density
θ	Heading angle of the wave

theory [3,4]. In order to deal with composite laminates, the CLPT (Classical Laminate Plate Theory) [5] can be used once the characteristic matrices of the laminate are calculated and is the simplest available theory.

More recently, some authors have proposed alternative methodologies for the calculation of the dispersion curves of more complex composite structures [6–10].

Among the finite-element based methods, the SFEM (Spectral Finite Element Method) is a wavenumber-based procedure which reformulates the wave propagation problem through a linear algebraic eigenproblem in the wavenumber space, assuming a three-dimensional displacement field within the plate [8–11].

The WFEM (Wave Finite Element Method) is also used similarly to the SFEM for obtaining the dispersion curves of homogeneous and periodic structures. The method makes use of the Bloch–Floquet theory, [12], and analyses the wave propagation in the media imposing the periodicity conditions to a single repetitive cell [12–18].

Both these procedures are affected by numerical conditioning when an heading angle, different from a few specific values, is imposed. For example, in the case of the WFEM, the polynomial eigenproblem, to be solved, when an general angle is imposed, might turn to a transcendental eigenvalue problem which is characterized by numerical instabilities and eigenvalue tracking issues, [16]. Moreover, it is fundamental determining which solutions of the eigenvalue problem are artefacts of the spatial discretization and which are valid estimates of wavenumbers in the continuous structure, [14,19,20].

The tracking of eigenwaves, performed through a Wave Assurance Criterion, [14,21], is a time-consuming task and it does not assure correct and robust results for two dimensional waveguides. Other issues of the method are associated with the periodicity effects: the solution scheme gives the same result for the wave modes and the frequencies of the propagation constants with period 2π, because of the spatial periodicity, giving rise to aliasing effects, [16].

On the other hand, the wave propagation in curved waveguides, i.e. cylinders and cones, is deeply analysed in the literature [22–26]. The propagation of longitudinal and flexural waves in axial-symmetric circular cylindrical shells with

periodic circular axial curvature is studied using a finite element method in [27]. The waves in thin uniform cylindrical shells, periodically stiffened by uniform circular frames of general cross-section, is analysed in [22]. Modern methods appeared continuously in the literature, for curved structures, both for the free wave propagation and the forced response [28,29].

A wave-based methodology for the free and forced analysis of the circumferential wave propagation of axial-symmetric structures, whatever they complexity and tapering, is proposed in [29].

Differently, some attempts to use a finite model to gather informations of an infinite waveguide are present in literature, with success in the identification of the periodic structural band-gaps [30,31].

The issues of having a correct mathematical formulation for the out-of-resonance wave-mode duality is analysed and discussed by Langley in [32]. It is stated and proved that, at least in the case of a 1D wave propagation, in a resonance condition a mode can be represented using a wave description [32].

To authors knowledge, very few works, dealing with a full representation of the dispersion curves of the periodic (or homogeneous) waveguide, are present in literature and, in this work, an alternative approach is proposed which allows to overcome all the numerical instabilities. The approach produces results for every heading angle, through a simple real modal analysis of a cylindrical equivalent finite element model, performable with any available in-house or commercial code.

The paper is structured as follows: Section 2 gives an overview of all the reference solutions adopted; Section 3 describes the analogy proposed and Section 4 contains the analytic and numerical validations for all the analysed test-cases.

2. Reference solutions

In the following section an overview of the adopted reference solutions is given for isotropic beams and plates and for composite laminates.

2.1. Isotropic beam and plate

Considering a beam with E as the Young modulus, I the area moment of inertia, ρ the mass density and A the cross-sectional area; The phase wave speed in a flexural beam can be expressed a follows, [4,17,33]:

$$c_b = \left(\frac{EI}{\rho A}\right)^{1/4} \sqrt{2\pi f} \tag{1}$$

Similarly a uniform thin and flat plate is here considered, made of an homogeneous material. From classical thin plate theory, [4], three wave types propagate in the material of thickness h: longitudinal, shear and bending waves. Each of these is associated with the respective wavenumber: k_l, k_s, k_b.

$$k_l = 2\pi f \sqrt{\frac{\rho(1-\nu^2)}{E}} \quad k_s = 2\pi f \sqrt{\frac{2\rho(1+\nu)}{E}} \quad k_b = \sqrt{2\pi f}\left(\frac{\rho h}{D}\right)^{1/4} \tag{2}$$

where D is the well known flexural stiffness of the plate and ν the Poisson ratio. By using these relationships, any information for a predictive methodology can be gathered. For example, the discretization of the predictive finite element model could be designed to work up to a given excitation frequency, once the wavelengths are known.

2.2. The classical lamination theory (CLPT)

The basic analytic equations for a thin composite plate are here summarized. For a laminate, the relations between forces/moments and strain/curvatures can be written as, [5,11]:

$$\mathbf{N} = \mathbf{A}\boldsymbol{\epsilon}_0 + \mathbf{B}\boldsymbol{\gamma}_0 \qquad \mathbf{M}_l = \mathbf{B}\boldsymbol{\epsilon}_0 + \mathbf{D}\boldsymbol{\gamma}_0 \tag{3}$$

where ϵ_0 are the strains of the middle plane and γ_0 the curvatures of it.

A, **B** and **D** are the matrices which compose the well known matrices which depends on stress–strain relation of each lamina and the chosen layup sequence [5,11].

$$\boldsymbol{\epsilon}_0 = \begin{bmatrix} \dfrac{\partial u}{\partial x} \\ \dfrac{\partial v}{\partial y} \\ \dfrac{\partial u}{\partial y} + \dfrac{\partial v}{\partial x} \end{bmatrix} \tag{4}$$

$$\boldsymbol{\gamma}_0 = \begin{bmatrix} -\dfrac{\partial^2 w}{\partial x^2} \\ -\dfrac{\partial^2 w}{\partial y^2} \\ -2\dfrac{\partial^2 w}{\partial y \partial x} \end{bmatrix} \tag{5}$$

where u and v are the in-plane displacements, while w is the out-of-plane displacement. Following the procedure explained in [5], a 3D displacements wave is assumed to propagate along the plate:

$$\begin{bmatrix} u \\ v \\ w \end{bmatrix} = \begin{bmatrix} U \\ V \\ W \end{bmatrix} e^{\mathrm{j}[k(\cos(\theta)x + \sin(\theta)y) - \omega t]} \tag{6}$$

where θ is the heading angle of the wave and U, V, W the displacement field variables. It is possible to converge to a polynomial problem in k (the wavenumber).

The following expressions can be used to compute the wavenumbers of the laminated waveguide, once the material is chosen, [5,11].

$$k_b(\theta, f) = \sqrt{2\pi f}\left(\frac{\rho_s}{\mathbf{P}^T \mathbf{D} \mathbf{P}} \right)^{1/4} \tag{7}$$

$$k_s(\theta, f) = 2\pi f \sqrt{\frac{\rho_s}{\eta_s(\theta)}} \tag{8}$$

$$k_l(\theta, f) = 2\pi f \sqrt{\frac{\rho_s}{\eta_l(\theta)}} \tag{9}$$

where:

$$\mathbf{P}^T = \begin{bmatrix} \cos(\theta)^2 & \sin(\theta)^2 & 2\sin(\theta)^2 \cos(\theta)^2 \end{bmatrix} \tag{10}$$

$$\mathbf{L} = \begin{bmatrix} \cos(\theta) & 0 \\ 0 & \sin(\theta) \\ \sin(\theta) & \cos(\theta) \end{bmatrix} \tag{11}$$

η_l and η_s eigenvalues of the matrix $\mathbf{L}^T \mathbf{A} \mathbf{L}$.

3. The proposed analogy

The method, presented here, is based on the assumption that the free wave propagation in an infinite flat media, i.e. a panel, can be also described considering a free wave propagation along a circumferential path. In fact, in a local reference system which follows the geometrical (circumferential; Fig. 1) path, the waves are free to propagate in analogy to what they do in the case of the equivalent infinite flat structure. The finiteness of the circular structure does not affect the wave propagation since no impedance variations are encountered running in loop along the curved path. Equivalently, this is a way to describe an infinite periodic condition, in a local coordinate system, as resulting from the Bloch–Floquet theorem [12,17]. The difference stands in its implicit geometrical definition through a finite circular structure, instead of explicitly defining a propagation relation on a reference line. In a periodic waveguide, the link between a wavefield Γ (displacement, velocity, force, etc.), at two points x and $x + \Delta_x$, is given by complex propagating constants, [12,17]:

$$\Gamma(x + \Delta_x, f) = \Gamma(x, f) e^{\mathrm{j}\Delta_x k_n(f)} \tag{12}$$

where k_n is the wavenumber associated with the wavetype n and f the frequency. On the other hand, for a circumferential mode of order i, the field in two points is related, similarly, as follows:

$$\Gamma(\theta + \Delta_\theta, f) = \Gamma(x, f) e^{\mathrm{j}\Delta_\theta i/2\pi R} \tag{13}$$

where $i/2\pi R$ is the circumferential wavenumber associated with the mode of order i.

In a set of discrete (natural) frequencies, each specific circumferential mode is representative of the corresponding wavemode and Eq. (12) and (13) are equivalent. Figs. 1 and 2 illustrate the previous concepts.

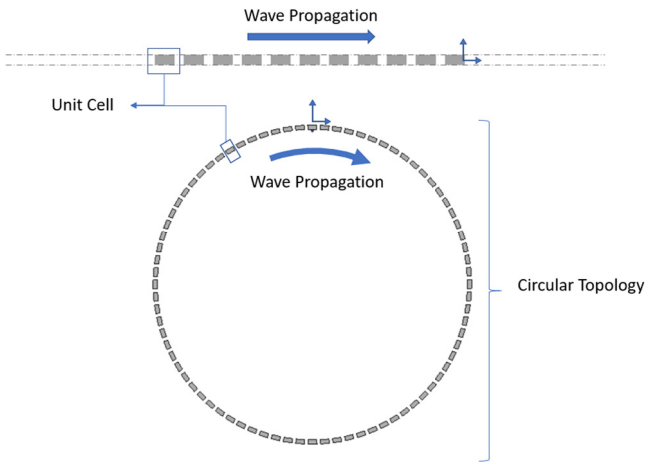

Fig. 1. The analogy proposed: (a) Free wave propagation along an infinite flat waveguide; (b) equivalence in a circular topology generated from the original model.

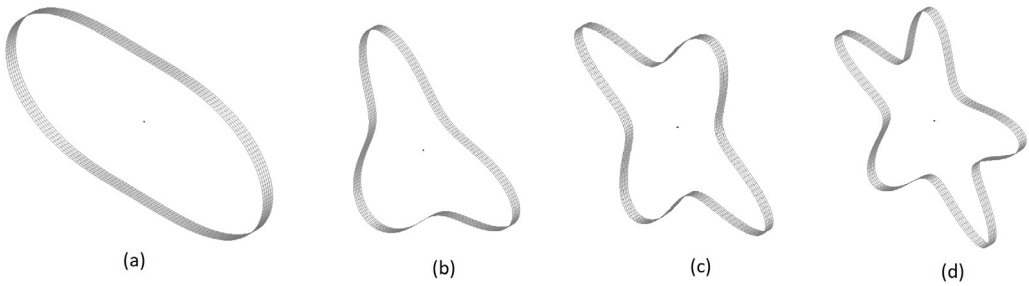

Fig. 2. Purely circumferential bending modes in a circular structure: (a) Circumferential Order = 2; (b) Circumferential Order = 3; (c) Circumferential Order = 4; (d) Circumferential Order = 5.

It is worth to emphasize that the aim of the approach is not related to the analysis of the waves in a cylindrical waveguide. The equivalent circular geometry is here used only to simulate a wave propagation in an infinite domain: in this way, the wave properties in an infinite panel (or beam) can be calculated working on the circumferential wave propagation in a finite circle.

A modal analysis (Eq. (14)) of cylinders or rings, built from the reference structure, gives a discrete set of frequencies (natural modal frequencies) where the modal circumferential wavelength represents the wave propagation in the infinite media. The dispersion curves of the laminate can be thus calculated in discrete points.

By using the equation of motion in discrete coordinates and assuming no external forces are applied to the system, the eigenvalue problem can be written as:

$$[\mathbf{K} - \omega^2 \mathbf{M}]\mathbf{q} = \mathbf{0} \tag{14}$$

where $\mathbf{q}$ is the nodal vector of degrees of freedom (DoFs); $\mathbf{K}$ and $\mathbf{M}$ are the stiffness and mass matrices. Damping can be modelled by including, in Eq. (14), appropriate complex matrices and/or coefficients. The operation is easily performable using any commercial FE software.

It is useful to remind the role of the modal wavelengths in rings; a purely circumferential mode for a circular structural model is in Fig. 2. Given a certain radii (R), in general, the wavelength associated to a given mode is given by:

$$\lambda_i = \frac{2\pi R}{i} \tag{15}$$

where i is the order of the circumferential mode and can be rawly identified in the number of lobes present in the modal deformed shape.

A key parameter is, here, the modal angular sampling factor, given by the ratio of the modal wavelength and the radii of the circumference: $2\pi/i$. Its importance, within the present method, is discussed in next section.

The modes of a finite structure describe a steady wave condition while the dispersion curves, for any structure, describe a wave propagation [32]. Any wave type propagating in an infinite media, can be described using this analogy. However, to correctly and easily identify the bending, shear and longitudinal wavemodes singularly, the circular waveguide can be

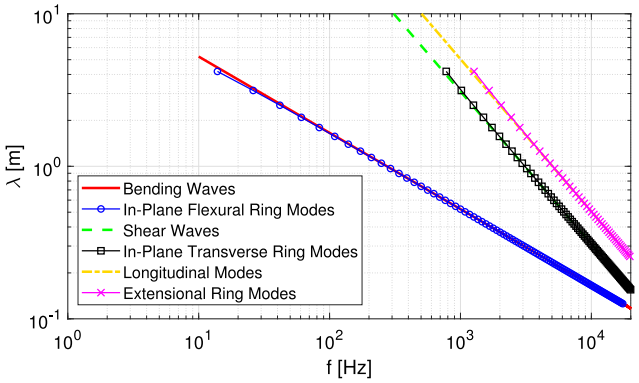

Fig. 3. Bending, shear and longitudinal wavemodes wavelength in an infinite beam and the corresponding beam–ring circumferential modes.

constrained, in a Finite Element Solution, in order to show only the desired circumferential wave types. For example, in the case of bending waves, the constraints of the cylindrical domain must allow only out-of-plane displacements and rotations. Similar considerations are applied for shear and longitudinal waves.

In summary, the proposed method is composed by the following sequential passages:

1. Generate a finite element model of the unit cell of the structure to be analysed, as usually done in a SFEM or WFEM framework (Fig. 1(a))
2. Generation of a circular topology using the elementary cell as a base. The radius and the number of elements has to be chosen in accordance to the target frequency band (Fig. 1(b))
3. Perform a modal analysis of the circular structure (Eq. (14))
4. Identify the wave branches and evaluate the circumferential wavenumbers (Eq. (15)) of the structural eigenmodes calculated at the previous step
5. Plotting the λ_i for each natural frequency and for each branch.

4. Validations

In the following section the validation of the proposed approach is performed for different test-cases.

4.1. Analytic validation: infinite beam and ring

A first test-case is the one of a beam. This is particularly convenient since both the bending wave speed of an infinite beam and the natural frequencies of a beam–ring can be calculated using analytic formulas. For every ring wavelength λ_i, where i is the circumferential order, the natural frequencies for bending, shear and longitudinal modes, respectively $f_{b,i}$, $f_{s,i}$ and $f_{n,i}$, are given by Blevins in [34]:

$$f_{b,i} = \frac{i(i^2-1)}{2\pi R^2 i}\left(\frac{EI}{\rho A}\right)^{1/4}; \quad f_{s,i} = \frac{\sqrt{i^2+1}}{2\pi R}\sqrt{G/\rho}; \quad f_{l,i} = \frac{\sqrt{i^2+1}}{2\pi R}\sqrt{E/\rho}; \tag{16}$$

with E as the Young modulus, G the shear modulus, I the moment of inertia, ρ the mass density and A the cross-sectional area.

In Fig. 3, a beam with rectangular section is used as a test-case and the results obtained with Eq. (1) and (16) are compared. The results show a very good agreement which validates the analogy proposed. The results introduce a range of validity of the approach starting from a specific value of the modal sampling factor (modal order). The accuracy of the proposed method is high enough starting from the sixth modal order and it is independent on the radii and length of the ring considered, as expected (Fig. 4).

4.2. Analytic validation: infinite cylinder ovaling modes

Another analytic validation is here proposed, using the natural ovaling modes of an infinite cylinder. The natural frequencies, for this specific modes of the infinite cylinder, can be calculated using the formulas proposed by Blevins in [34], here reported for completeness in Eq. (17). For every ring wavelength λ_i, where i is the circumferential order, the natural frequency $f_{n,i}$ is:

$$f_{n,i} = \frac{h}{2\pi R^2\sqrt{12}}\sqrt{\frac{E}{\rho(1-\nu^2)}}\frac{i(i^2-1)}{\sqrt{i^2+1}} \tag{17}$$

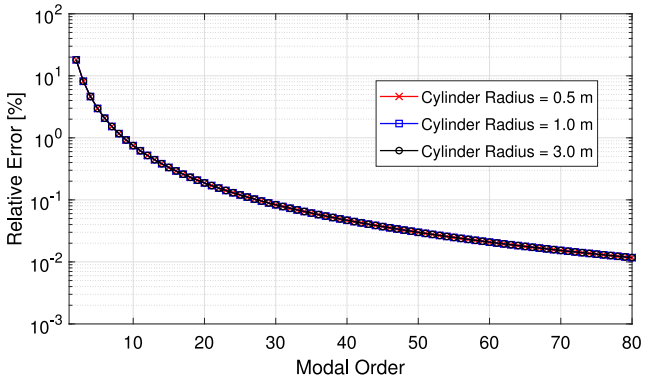

Fig. 4. Relative error (log-scale) between the bending wavelength in an infinite panel and the modal wavelengths of an infinite cylinder.

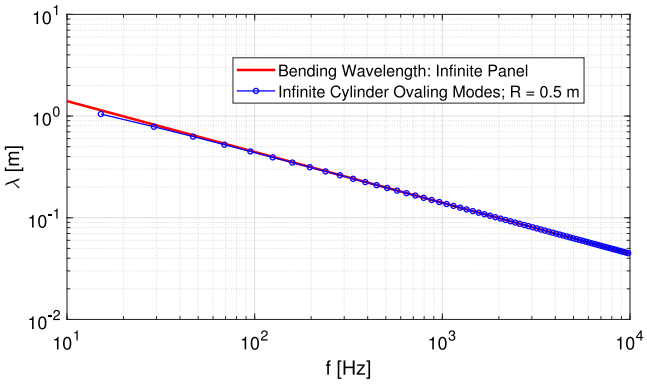

Fig. 5. Bending wavelength in an infinite panel and the ovaling modes of an infinite cylinder.

In Fig. 5, an infinite plate of thickness h is used as a test-case and the results obtained with Eq. (1) and (17) are compared for bending waves. The results show a very good agreement, validating the analogy proposed also for a higher order model. Moreover, again, the range of validity depends on the modal sampling factor. In Fig. 4, the relative error for this specific case is shown for different radii. The error, in percentage, is independent on the radii of the cylinder and is inferior to 2% starting from the sixth modal order, as found in the previous section.

4.3. Numerical validation: isotropic panel

A first validation with an isotropic aluminium material is performed: $E = 7.0 \times 10^{10}$ Pa, $\rho = 2750$ kg/m^3, $\nu = 0.33$. The analytic solution is used as a reference. In Fig. 6 a comparison of the infinite plate bending wavelength (versus frequency) with the results of a modal analysis on cylinders of different radii is shown. As in the case of the beam, the accuracy of the method is only dependent on the modal angular sampling factor; as soon as it reaches the unitary value, thus the sixth modal order is reached, the relative error of the present method is inferior to 2%. This is illustrated more specifically in the case of laminates, comparing the error for every heading angle.

Depending on the value of R, the region of accuracy moves with the frequency, approaching higher bands when R lowers, and vice-versa, since any modal order shifts with the frequency.

Depending on the discretization adopted, the accuracy method can strongly vary. Two cases are here analysed: fixed radii R (Fig. 7) and fixed element size Δ_X (Fig. 8).

In the first case the question moves to a classic sampling problem. Given a number of elements (N_{el}), through which the circumference is discretized, assuming, as a rule of thumb, at least four elements per wavelength as an acceptable approximation (six or ten are, in general, preferred), the maximum modal order predicted is given by the integer of the ratio $N_{el}/4$. The error starts increasing up to modal order $N_{el}/2$ before diverging (Fig. 9).

On the other hand, keeping the element size fixed and increasing the number of elements means increasing the circumference radii R (Fig. 10). The expected effect is a frequency shift of the validity region, in the wavenumber domain, when moving from one case to the other, as in Fig. 10.

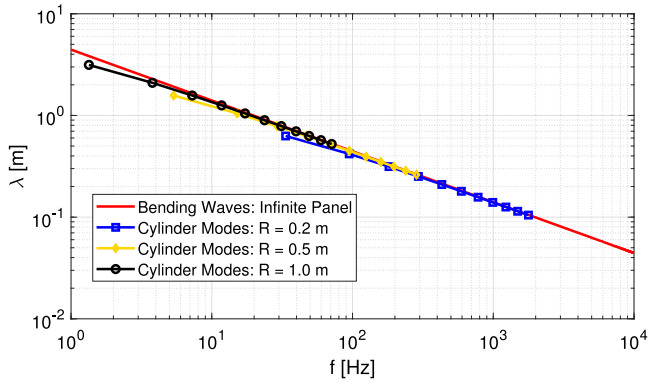

Fig. 6. Isotropic uniform plate: infinite panel solution and the circumferential modes of a cylindrical finite structure made of plate elements.

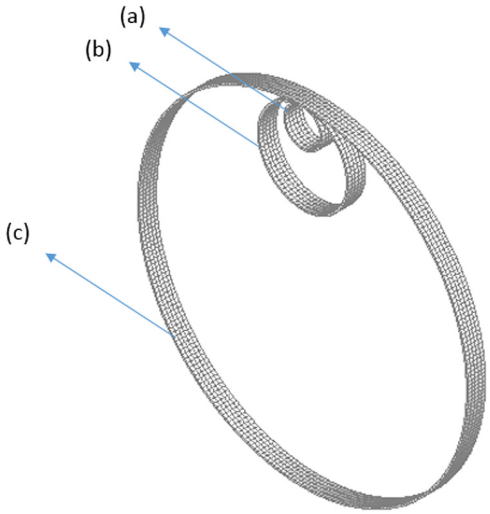

Fig. 7. Comparison for increasing number of elements for a given element size . (a) 32, (b) 80, (c) 300 elements.

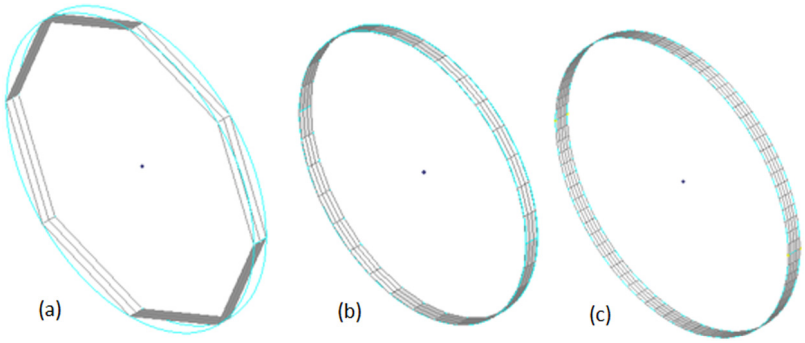

Fig. 8. Comparison for increasing number of elements for a given circumference radii *R*. From the left side: 8, 32, 80 elements.

4.4. Laminated panel

An heading angle can be specified in order to analyse the wave propagation in a specific direction (Fig. 11). In this solutions scheme, the problem is never ill-conditioned and can be normally solved with a simple real modal analysis, independently on the value of the angle itself. The graphite-epoxy lamina elastic properties, used in the present work, are in Table 1. The thickness of each lamina is 1 mm.

Table 1
Lamina elastic properties and stacking sequence.

$E_1 1$	$E_2 2$	G_{12}	ν_{12}	Layup
125 GPa	12.5 GPa	6.89 GPa	0.38	[90°, 0°, 0°, 0°, 90°]

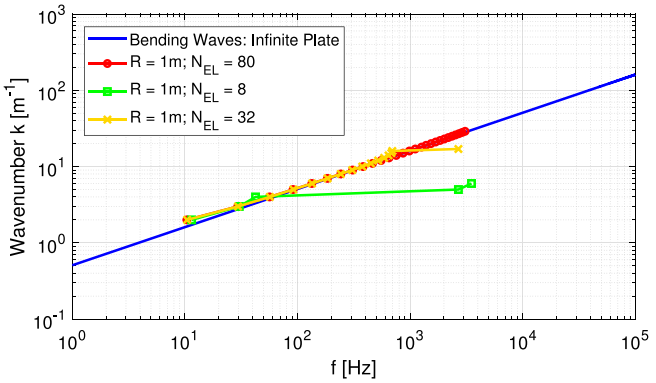

Fig. 9. Effect of the mesh: comparison for increasing number of elements for a given circumference radii R (isotropic panel). Elements size variable.

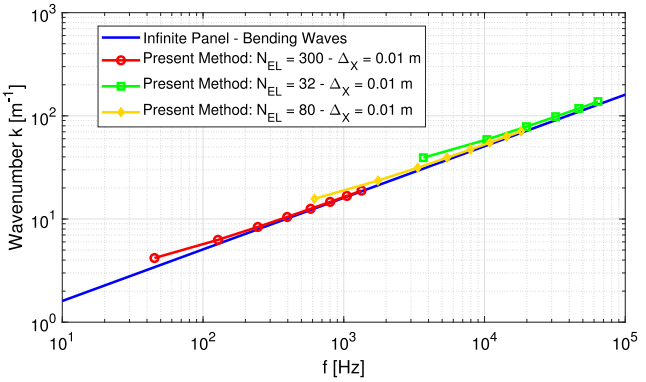

Fig. 10. Effect of the mesh: comparison for increasing number of elements for a given element size (isotropic panel). Circumference radii R variable: Fig. 7(a) 0.05 m, Fig. 7(b) 0.13 m, Fig. 7(c) 0.48 m.

In the framework of the present approach, a cut-on wavenumber can be defined; below this value, a cylinder with radii R, has no predictive capability. In general, given a certain radii R the cut-on wavenumber can be defined from the smallest modal order ($i = 2$): $2/R$. This aspect has an impact only for bending waves, as evident in Figs. 12–14, where, in addition, the accuracy of the method is shown also for shear and longitudinal wave types. Increasing the size of the radii, this limit moves to lower wavenumbers and frequencies.

As previously stated, the accuracy of the method is only dependent on the modal angular sampling factor, and, when it reaches the unitary value, the accuracy is acceptable as in Fig. 15, where the relative errors are compared. For a modal order superior to the fifth, the relative error is inferior to 2% and keeps lowering for increasing the frequency, as found in all previous test-cases.

The great advantage is in the ease of use and the possibility to arbitrarily choose an heading angle, without taking care about the eventual ill-conditioning of the mathematical problem, [11,14,16]. Moreover, the eigenvalue tracking is no more needed since any wave type evolves singularly if specific boundary conditions are imposed to the finite cylinder before the modal analyses, as previously discussed. In Fig. 16 a pattern of bending wavenumbers is calculated, for a specific frequency, with the present method, and compared to the one obtained using the CLPT.

Once a modal analysis is performed, the modal shapes can be extracted straightforwardly. A better way to visualize the mode shapes, will be the stretching of the circumferential modes along a rectilinear path. In Fig. 17 a fourth order mode has been chosen and the mode shapes are visualized for bending, shear and longitudinal wave types, along the circular model. On the other hand, in Fig. 18, the same modes are visualized in a rectified model.

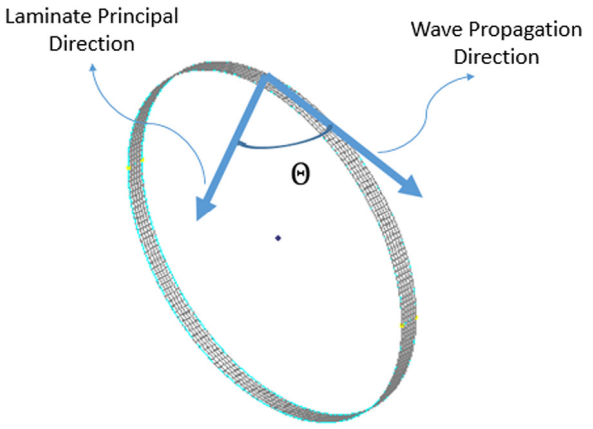

Fig. 11. Scheme of the laminate heading angle with respect to the wave propagation direction.

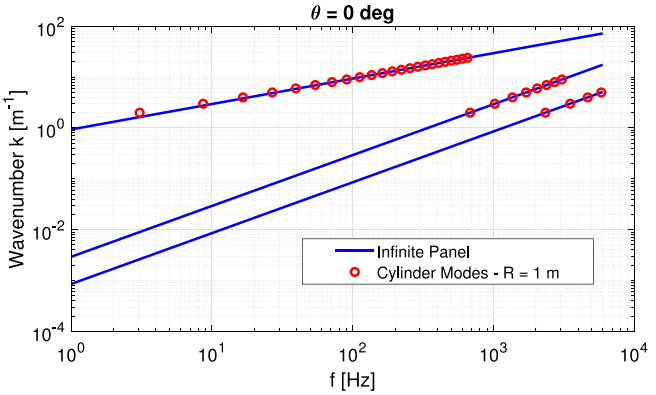

Fig. 12. Dispersion curves of the laminate panel; heading angle 0°. CLPT results used as a reference.

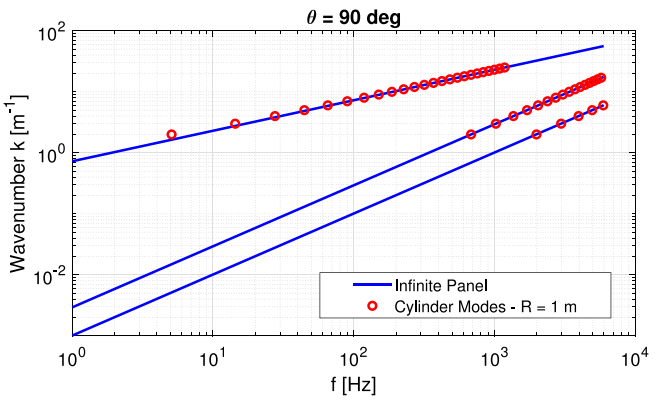

Fig. 13. Dispersion curves of the laminate panel; heading angle 90°. CLPT results used as a reference.

4.5. Complex structural shapes

In order to prove the accuracy of the analogy, even for non-homogeneous structures and large heterogeneity scales, an aluminium-made double-wall panel with mechanical connections is used as a test-case (Fig. 19). A wave finite element method (WFEM) is used for obtaining the reference results [16,18,29]. Fig. 20 shows the comparison among the modes generated by the cylindrical model ($R = 0.4$ m), built from the elementary cell representing the reference waveguide, and

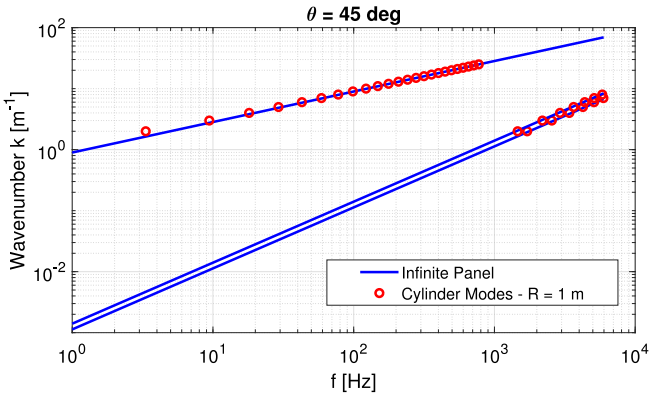

Fig. 14. Dispersion curves of the laminate panel; heading angle 45°. CLPT results used as a reference.

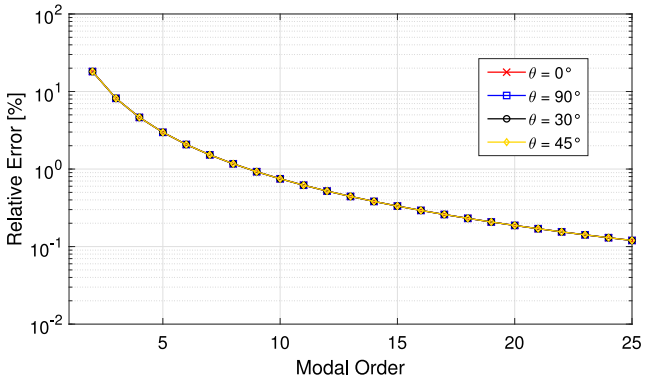

Fig. 15. Relative errors (log-scale) for different heading angles (bending waves). The CLPT results used as reference.

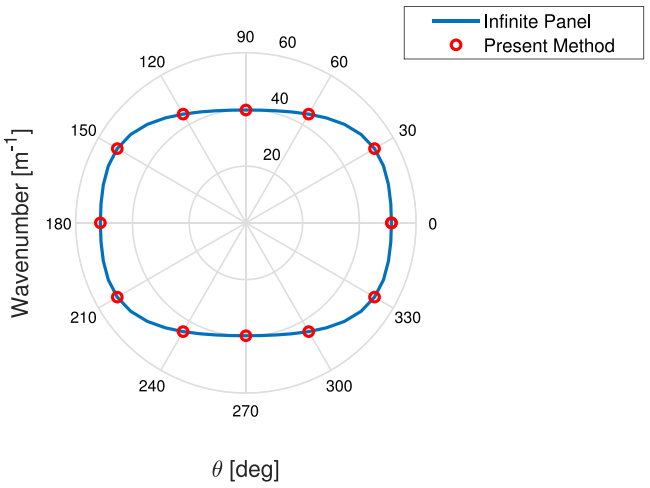

Fig. 16. Pattern of the bending wavenumbers for the laminate plate analysed; 3000 Hz.

the flat infinite reference waveguide. In this case only bending waves have been analysed. Even in this complex case the agreements is excellent above the sixth modal order.

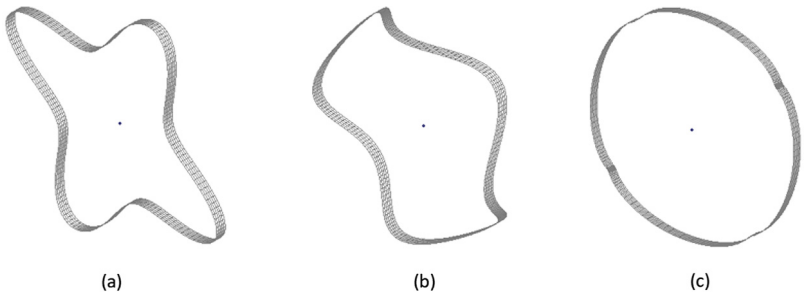

Fig. 17. Purely circumferential modes in a laminate infinite panel; X–Y as cross sectional plane. Fourth circumferential mode - (a) Bending: 16.6 Hz; (b) Shear: 1364 Hz; (c) Longitudinal: 4674 Hz.

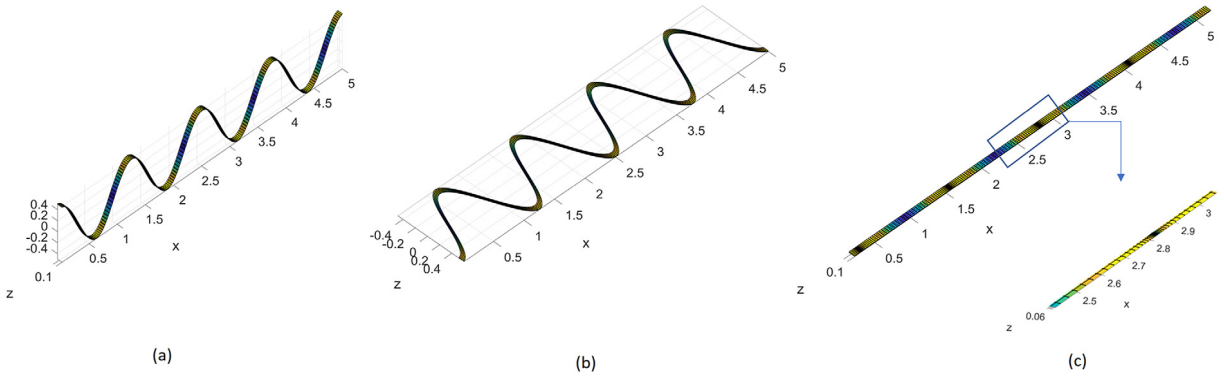

Fig. 18. Rectified circumferential modes in a laminate infinite panel; X–Y as cross sectional plane. Fourth circumferential mode - (a) Bending: 16.6 Hz; (b) Shear: 1364 Hz; (c) Longitudinal: 4674 Hz.

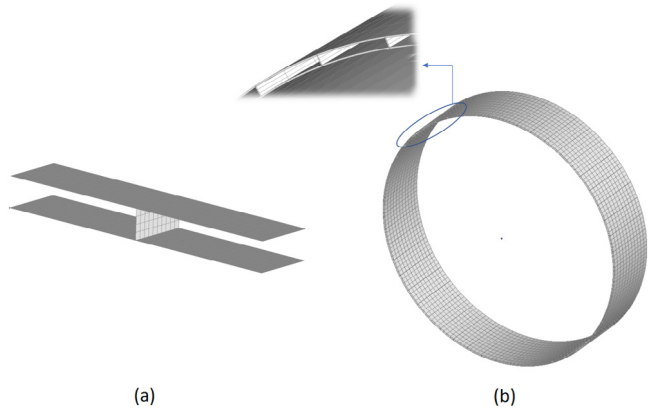

Fig. 19. A double-wall panel with mechanical connection: (a) Elementary FE Cell; (b) Cylindrical Model.

5. Conclusions

The proposed analogy proved to be accurate and robust in predicting the dispersion curves of beams and plates through a simple modal analysis of a cylindrical finite element model. The calculations are always well-conditioned for every heading angle chosen, differently from most of the methods present in literature. The results are accurate and the relative error is independent on the cylinder axial length and radii (R). A test on a double-wall panels with mechanical connections shows how the features of the method are applicable also to complex structural shapes.

The predictive region can be easily trimmed using different values of the curvature or, instead, using a high value of R and a fine mesh in order to be able to move from low (low cut-on wavenumber) to high frequencies. The computational

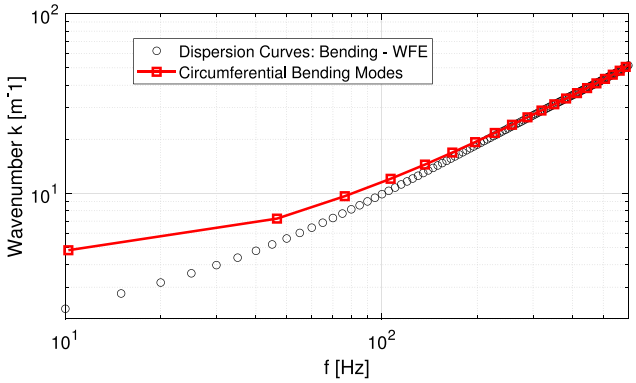

Fig. 20. Bending Waves for the double-wall panel with mechanical connection. Numerical comparison between the WFEM and the present analogy.

cost associated with such meshes, especially for a simple real modal analysis, is not a relevant parameter and, moreover, the numerical conditioning is null.

A generic FE-based code can be used for the purpose and both plate and solid elements have been tested and validated for the accuracy of the results. Again, it must be highlighted that for bending motion, the results start to have an acceptable accuracy (lower than 2%) starting from the fifth modal order. A correct mesh size is required to avoid aliasing problems at higher frequencies.

Further developments might be related to the possibility of predicting also coupled wave-types which arise to higher frequencies and the possibility to include global and through-thickness damping.

Acknowledgments

This project has received funding from the European Union's Horizon 2020 research and innovation program, Italy under the Marie Sklodowska-Curie grant agreement No. 675441. The author would like to gratefully acknowledge everyone involved in the VIPER project. Discussions with Dr. Petrone are gratefully acknowledged.

References

[1] R. Cook, D. Malkus, M. Plesha, R. Witt, Concepts and Applications of Finite Element Analysis, John Wiley & Sons Inc, 2001.
[2] L. Cremer, M. Heckl, B. Petersson, Structure-Borne Sound - Structural Vibrations and Sound Radiation at Audio Frequencies, Springer, 2005, http://dx.doi.org/10.1007/b137728.
[3] A. Love, The small free vibrations and deformation of a thin elastic shell, Philos. Trans. R. Soc. Lond. Ser. A Math. Phys. Eng. Sci. 179 (1888) 491–546, http://dx.doi.org/10.1098/rsta.1888.0016.
[4] A. Leissa, Vibration of Plates, vol. 160, Scientific and Technical Information Division, National Aeronautics and Space Administration, 1969.
[5] R. Jones, Mechanics of Composite Materials, Taylor & Francis, 1999.
[6] B. Mace, D. Duhamel, M. Brennan, L. Hinke, Finite element prediction of wave motion in structural waveguides, J. Acoust. Soc. Am. 117 (2005) 2835–2843, http://dx.doi.org/10.1121/1.1887126.
[7] P. Shorter, Wave propagation and damping in linear viscoelastic laminates, J. Acoust. Soc. Am. 115 (2004) 1917–1925, http://dx.doi.org/10.1121/1.1689342.
[8] M. Chitnis, Y. Desai, T. Kant, Wave propagation in laminated composite plates using higher order theory, J. Appl. Mech. 68 (3) (2001) 503–505, http://dx.doi.org/10.1115/1.1352062.
[9] A. Baz, Spectral finite-element modelling of the longitudinal wave propagation in rods treated with active constrained layer damping, Smart Mater. Struct. 9 (2000) 372–377, http://dx.doi.org/10.1088/0964-1726/9/3/319.
[10] A. Chakraborty, S. Gopalakrishnan, A spectral finite element model for wave propagation analysis in laminated composite plate, J. Vib. Acoust. 128 (4) (2006) 477–488, http://dx.doi.org/10.1115/1.2203338.
[11] E. Barbieri, A. Cammarano, S. De Rosa, F. Franco, Waveguides of a composite plate by using the spectral finite element approach, J. Vib. Control 15 (3) (2009) 347–367, http://dx.doi.org/10.1177/1077546307087455.
[12] L. Brillouin, Wave Propagation in Periodic Structures: Electric Filters and Crystal Lattices, second ed., Dover Publications, Mineola, New York, 1953, http://dx.doi.org/10.1016/S0031-8914(53)80099-6.
[13] Y. Waki, B. Mace, M. Brennan, Numerical issues concerning the wave and finite element method for free and forced vibrations of waveguides, J. Sound Vib. 327 (2009) 92–108, http://dx.doi.org/10.1016/j.jsv.2009.06.005.
[14] C. Droz, C. Zhou, M. Ichchou, J.-P.. Laine, A hybrid wave-mode formulation for the vibro-acoustic analysis of 2d periodic structures, J. Sound Vib. 363 (2016) 285–302, http://dx.doi.org/10.1016/j.jsv.2015.11.003.
[15] C. Droz, J.-P.. Laine, M. Ichchou, G. Inquiete, A reduced formulation for the free-wave propagation analysis in composite structures, Compos. Struct. 113 (2014) 134–144, http://dx.doi.org/10.1016/j.compstruct.2014.03.017.
[16] E. Manconi, B.R. Mace, Modelling wave propagation in two dimensional structures using finite element analysis, J. Sound Vib. 318 (45) (2008) 884–902, http://dx.doi.org/10.1016/j.jsv.2008.04.039.
[17] D. Mead, Wave propagation in continuous periodic structures: research contributions from southampton, J. Sound Vib. 190 (3) (1996) 495–524, http://dx.doi.org/10.1006/jsvi.1996.0076.

[18] J. Morsbol, S. Sorokin, Elastic wave propagation in curved flexible pipes, Int. J. Solids Struct. 75–76 (2015) 143–155, http://dx.doi.org/10.1016/j.ijsolstr.2015.08.009.
[19] D. Chronopoulos, B. Troclet, O. Bareille, M. Ichchou, Modeling the response of composite panels by a dynamic stiffness approach, Compos. Struct. 96 (2013) 111–120, http://dx.doi.org/10.1016/j.compstruct.2012.08.047.
[20] D. Chronopoulos, M. Ichchou, B. Troclet, O. Bareille, Computing the broadband vibroacoustic response of arbitrarily thick layered panels by a wave finite element approach, Appl. Acoust. 77 (2014) 89–98, http://dx.doi.org/10.1016/j.apacoust.2013.10.002.
[21] D. Magliacano, M. Ouisse, A. Khelif, S. De Rosa, F. Franco, N. Atalla, Validation of the shift cell approach for the modelling of acoustic properties of porous materials embedding periodic inclusions, Novem2018 Conference, Balearic Islands, Spain.
[22] D.J. Mead, N.S. Bardell, Free vibration of a thin cylindrical shell with periodic circumferential stiffeners, J. Sound Vib. 115 (3) (1987) 499–520, http://dx.doi.org/10.1016/0022-460X(87)90293-8.
[23] R. Langley, Wave motion and energy flow in cylindrical shells, J. Sound Vib. 169 (1) (1994) 29–42, http://dx.doi.org/10.1006/jsvi.1994.1004.
[24] J.M. Renno, B.R. Mace, Calculating the forced response of cylinders and cylindrical shells using the wave and finite element method, J. Sound Vib. 333 (21) (2014) 5340–5355, http://dx.doi.org/10.1016/j.jsv.2014.04.042.
[25] S. Markus, D. Mead, Axisymmetric and asymmetric wave motion in orthotropic cylinders, J. Sound Vib. 181 (1) (1995) 127–147, http://dx.doi.org/10.1006/jsvi.1995.0130.
[26] F. Honarvar, E. Enjilela, A.N. Sinclair, S.A. Mirnezami, Wave propagation in transversely isotropic cylinders, Int. J. Solids Struct. 44 (16) (2007) 5236–5246, http://dx.doi.org/10.1016/j.ijsolstr.2006.12.029.
[27] A. Ghoshal, M. Accorsi, M. Bennett, Wave propagation in circular cylindrical shells with periodic axial curvature, Wave Motion 23 (1996) 339–352, http://dx.doi.org/10.1016/0165-2125(95)00056-9.
[28] B. Liu, Y. .Xing, M. Qatu, A. Ferreira, Exact characteristic equations for free vibrations of thin orthotropic circular cylindrical shells, Compos. Struct. 94 (2) (2012) 484–493, http://dx.doi.org/10.1016/j.compstruct.2011.08.012.
[29] F. Errico, M. Ichchou, S. De Rosa, O. Bareille, F. Franco, The modelling of the flow-induced vibrations of periodic flat and axial-symmetric structures with a wave-based method, J. Sound Vib. 424 (2018) 32–47, http://dx.doi.org/10.1016/j.jsv.2018.03.012.
[30] M. Brun, G. Giaccu, A. Movchan, N. Movchan, Asymptotics of eigenfrequencies in the dynamic response of elongated multi-structures, Proc. R. Soc. A 468 (2012) 378–394, http://dx.doi.org/10.1098/rspa.2011.0415.
[31] M. Brun, A. Movchan, I. Jones, Phononic band gap systems in structural mechanics: finite slender elastic structures and infinite periodic waveguide, J. Vib. Acoust. 135 (2013),http://dx.doi.org/10.1115/1.402381.
[32] R.S. Langley, Some perspectives on wave-mode duality in SEA, in: IUTAM Symposium on Statistical Energy Analysis, 1999, pp. 1–12, http://dx.doi.org/10.1007/978-94-015-9173-7_1.
[33] V. D'Alessandro, Investigation and Assessment of the Wave and Finite Element Method for Structural Waveguides (Ph.D. thesis), University of Naples Federico II, 2014, URL http://www.fedoa.unina.it/9931/.
[34] R. Blevins, Formulas for Natural Frequency and Mode Shape, Krieger, Malabar, Florida, 1979, http:/dx.doi.org/10.1121/1.384246.